JOURNAL OF COMPUTATIONAL PHYSICS 97, 53–72 (1991)

High Resolution Schemes for Steady Flow Computation

Z. WANG AND B. E. RICHARDS

Department of Aerospace Engineering, University of Glasgow, Glasgow G12 8QQ, Scotland, United Kingdom

Received September 7, 1989; revised May 9, 1990

With the introduction of the concept of total variation diminishing scheme (TVD), a variety of numerical schemes using this approach have emerged. For steady state calculations, two particular TVD schemes have proved popular, i.e., the Yee symmetric and the Osher–Chakravarthy upwind TVD schemes. When applied to Euler equations, these two schemes give almost identical results. However, when they are employed to solve Navier–Stokes equations, the authors found dramatic differences especially when high Reynolds number viscous flow is tackled. In one viscous flow calculation, the Yee scheme gave an "unrepresentative" result while Osher–Chakravarthy scheme gave the "physical" result. The paper demonstrates that the numerical dissipation embedded in the schemes may be the cause. Modifications, therefore, are suggested to make Yee's scheme less dissipative so that it is much more suitable for viscous flow calculations. The numerical experiments do favor the modified scheme. Osher–Chakravarthy TVD scheme and the modified Yee scheme are recommended for viscous flow calculation at high Reynolds number.

1. INTRODUCTION

Considerable progress has been made in the numerical computation of compressible flow as a result of the development of more efficient, robust methods for solving the Euler and Navier–Stokes equations. Amongst others, the development of total variation diminishing (TVD) schemes [1] has constituted one of the major thrusts forward in CFD. Although TVD schemes are designed for transient applications, they also have been applied to steady state problems with great success. It is well known that even if explicit schemes are easy to implement, they suffer severe restrictions in the choice of time step and thus are less efficient than their implicit counterparts. It is also true that it is inappropriate to extend the second-order Lax–Wendroff method to implicit schemes because the steady state is found to depend on the time step. This paper addresses only steady state calculations, so only acceptable implicit schemes are considered. Osher and Chakravarthy [3] derived a family of high-order upwind TVD schemes whcih can be third-order accurate. More recently, Yee [4] generalized the works of Davis [5] and Roe [6] and introducecl thc concept of the symmetric TVD scheme, which in some cases is easier to implement than the Osher–Chakravarthy family. All these schemes have the property of avoiding spurious oscillations near sharp gradients and thus have

0021-9991/91 $3.00

been proved to be very robust for hypersonic problems with strong discontinuities such as shock waves, etc. Numerical experiments choosing the one-dimensional inviscid flow problem demonstrated that these schemes have the capacity to give high resolution for shock waves and have the advantage of giving satisfactory solutions on coarse grids. A straight extension of this approach of applying the one-dimensional scheme for each direction in multidimensional problems also has given quite satisfactory results. Comparisons have been made between a variety of the different TVD schemes [4, 7]. The conclusion is that they are almost identical in their shock capturing abilities when applied to inviscid flow computations. However, much still has to be done to test their capacities for resolving the viscous shear layer especially in multidimensional cases. This paper outlines work carried out by the authors to advance this topic. Early tests showed that dramatic differences were found especially when viscous solutions with high Reynolds number are sought. It has been found that the Yee symmetric TVD scheme has more dissipation than is required to resolve the viscous boundary layer, whereas the Osher–Chakravarthy TVD scheme gave far better resolution of the viscous shear layer. It was the investigation of the differences between these two schemes that resulted in the work of this paper.

The layout of this paper will be as follows. In Section 2, Harten's TVD concept and the sufficient conditions for both explicit and impliciet schemes to be TVD are reviewed. Then this set of conditions are used to derive a general TVD scheme and a principle of constructing upwind-biased second-order TVD scheme is developed. In Section 3, both the Osher–Chakravarthy and the Yee schemes are checked to see that they are TVD schemes. Comparisons are made which showed that the Yee TVD scheme is more dissipative than the Osher–Charkravarthy TVD schemes. Modifications to make Yee's scheme less dissipative are suggested. In Section 4, some results obtained from the application of these schemes in both inviscid and viscous flow calculations are discussed. Conclusions arising from the study are given in Section 5.

2. Review of TVD Concept and a Generalization Form TVD Scheme

Consider the scalar hyperbolic conservation law

$$\frac{\partial u}{\partial t}+\frac{\partial f(u)}{\partial x}=0, \qquad u(x,0)=u_0(x), \tag{2.1}$$

where f is called the flux and $a(u)=\partial f/\partial u$ is the characteristic speed. A general explicit and implicit scheme in conservative form can be written

$$u_j^{n+1}+\lambda\eta(h_{j+1/2}^{n+1}-h_{j-1/2}^{n+1})=u_j^n-\lambda(1-\eta)(h_{j+1/2}^n-h_{j-1/2}^n), \tag{2.2}$$

where $0\leqslant\eta\leqslant 1$, $\lambda=\Delta t/\Delta x$, with Δt the time step, and Δx the mesh size. Here u_j^n is a numerical solution of (2.1) at $x=j\,\Delta x$ and $t=n\,\Delta t$, $h_{j+1/2}=$

$h(u_{j-1}, u_j, u_{j+1}, u_{j+2})$, and h is a numerical flux function consistent with the conservation law in the following sense:

$$h(u_j, u_j, u_j, u_j) = f(u_j). \tag{2.3}$$

When $\eta = 0$, (2.2) reduces to an explicit scheme. When $\eta \neq 0$, (2.2) is an implicit scheme. For example, if $\eta = \frac{1}{2}$, the time differencing is the trapezoidal formula, and if $\eta = 1$, the time differencing is the backward Euler method.

It is commonly known that any weak solution of (2.1) has a non-increasing variation. When a numerical solution is sought, we also require that the variation of the discretised solution is diminishing. The total variation, $\mathrm{TV}(u^{n+1})$, of the solution is defined by

$$\mathrm{TV}(u^{n+1}) = \sum_j |u_{j+1}^{n+1} - u_j^{n+1}| \tag{2.4}$$

and so for total variation diminishing (TVD) schemes, the following condition must be satisfied:

$$\mathrm{TV}(u^{n+1}) \leqslant \mathrm{TV}(u^n). \tag{2.5}$$

If the numerical flux h in (2.2) is Lipschitz continuous then (2.2) can be written as

$$\begin{aligned} u_j^{n+1} - \lambda\eta(C_{j+1/2}\,\Delta u_{j+1/2} - D_{j-1/2}\,\Delta u_{j-1/2})^{n+1} \\ = u_j^n + \lambda(1-\eta)(C_{j+1/2}\,\Delta u_{j+1/2} - D_{j-1/2}\,\Delta u_{j-1/2})^n, \end{aligned} \tag{2.6}$$

where $\Delta u_{j+1/2} = u_{j+1} - u_j$, and $C_{j\pm 1/2}$, $D_{j\pm 1/2}$ are some bounded function of $\{u_j\}$. Harten further showed that sufficient conditions for (2.5) are

(a) if for all j,

$$\begin{gathered} \lambda(1-\eta)C_{j+1/2} \geqslant 0 \qquad \text{and} \qquad \lambda(1-\eta)\,D_{j+1/2} \geqslant 0 \\ \lambda(1-\eta)(C_{j+1/2} + D_{j+1/2}) \leqslant 1 \end{gathered} \tag{2.7a}$$

and

(b) if for all j,

$$-\infty < C \leqslant -\lambda\eta C_{j+1/2} \leqslant 0 \qquad \text{and} \qquad -\infty < C \leqslant -\lambda\eta D_{j+1/2} \leqslant 0 \tag{2.7b}$$

for some finite C.

For simplicity of discussion, we consider $c = \partial f/\partial u = \text{const}$, i.e., the linear wave equation

$$u_t + cu_x = 0, \qquad c > 0. \tag{2.8}$$

For steady state computations, the numerical flux function

$$h_{j+1/2} = \tfrac{1}{2}c(u_j + u_{j+1}) - \tfrac{1}{2}[1 - q(r_j)]\, c\, \Delta u_{j+1/2} \tag{2.9a}$$

is considered with

$$r_j = \frac{\Delta u_{j-1/2}}{\Delta u_{j+1/2}} \tag{2.9b}$$

and q is some function of r called a limiter. Several special schemes included in (2.9) are noted as follows. If $q(r) = 0$, the resultant scheme is a first-order upwind scheme. We call this limiter q^1. If $q(r) = 1$, the resultant scheme is a central difference second-order scheme (in space). Let this limiter be called q^c. If $q(r) = r$, the resultant scheme is upwind second order. Let this limiter be called q^u. If $q(r) = 2/3 + r/3$, the resultant scheme is third-order accurate. Let this limiter be called q^t.

According to the physics of wave propagation, only the upwind stream affects the current position. An upwind scheme, therefore, is highly desired in the wave modeling. In fact, any upwind-biased second-order scheme utilizing u_{j-2}, u_{j-1}, u_j, u_{j+1} is a weighted average of the central difference and upwind second-order scheme. So for any second-order scheme, the limiter should satisfy

$$\begin{aligned} q(r) &= \theta(r)\, q^c(r) + (1 - \theta(r))\, q^u(r) \\ &= \theta(r) + (1 - \theta(r))r = r + \theta(r)(1 - r) \end{aligned} \tag{2.10}$$

with $0 \leqslant \theta(r) \leqslant 1$, i.e., interpolation. Numerical experiments have shown that extrapolation causes over-compression and/or instability.

This family contains implicit as well as explicit schemes and, also, first- as well as second-order schemes. As a result of the fact that the time difference and space difference are discretised separately, they also have the advantage that the solution is independent of the time step and that the order of accuracy in space is solely decided by the numerical flux functions when the steady state is achieved. Now we further look into the numerical flux function (2.9a). When (2.9) is substituted into (2.2), the first term contributes to the discretization of $\Delta xc\, \partial u/\partial x$ to second-order accuracy without any numerical dissipation. The second term acts as a numerical dissipation term. When $q(r) < 0$, the scheme would be more dissipative than the first-order scheme. When $q(r) > 1$, some negative dissipation is added so that waves are usually compressed by the scheme. Possible non-physical solutions would result. It is noticed that when $q(r) = 1$ (i.e., central difference) no additional numerical dissipation is embedded in the scheme. This is a very desirable property when it is used to model the viscous flows at high Reynolds number. In fact, Eq. (2.9) can be rewritten in the form as (2.6) with

$$C_{j+1/2} = 0, \qquad D_{j-1/2} = c[1 + \tfrac{1}{2}q(r_j)/r_j - \tfrac{1}{2}q(r_{j-1})]. \tag{2.11}$$

Now sufficient conditions for (2.9) to be TVD are

$$1 + \tfrac{1}{2}q(r_j)/r_j - \tfrac{1}{2}q(r_{j-1}) \geqslant 0 \tag{2.12a}$$

and

$$c\lambda(1-\eta)[1 + \tfrac{1}{2}q(r_j)/r_j - \tfrac{1}{2}q(r_{j-1})] \leqslant 1. \tag{2.12b}$$

If we let

$$\begin{aligned} &q(r_j) = 0, \qquad \text{if} \quad r_j < 0 \\ &q(r_j) > 0, \qquad \text{otherwise.} \end{aligned} \tag{2.13}$$

Then we always have

$$q(r_j)/r_j \geqslant 0. \tag{2.14}$$

Under these conditions, the following sufficient conditions are obtained

$$\begin{aligned} &0 \leqslant q(r_j) \leqslant 2 \\ &0 \leqslant q(r_j)/r_j \leqslant \frac{2}{\lambda c(1-\eta)} - 2. \end{aligned} \tag{2.15}$$

Let

$$\frac{2}{\lambda c(1-\eta)} - 2 = k. \tag{2.16}$$

We should always have

$$k \geqslant 0; \text{ i.e., } \lambda \leqslant \frac{1}{c(1-\eta)}. \tag{2.17}$$

Figure 1 shows the TVD region with $\alpha = \tan^{-1}(k)$. Also displayed are the q functions needed to give the central difference and upwind second-order schemes and the third-order scheme. It is clear that for any upwind-biased second-order schemes, their limiters should lie between the two lines $q = 1$ and $q = r$. We notice that the following limiter will give the most compressive second-order TVD scheme:

$$q(r) = \begin{cases} 0, & r \leqslant 0 \\ kr, & 0 < r \leqslant 1/k \\ 1, & 1/k < r \leqslant 1 \\ r, & 1 < r \leqslant 2 \\ 2, & r > 2. \end{cases} \tag{2.18}$$

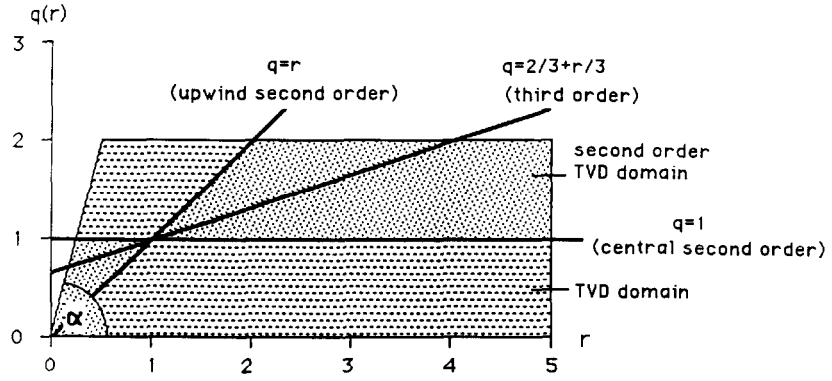

FIG. 1. TVD domain.

In fact, this limiter is an analogue of Roe's Superbee in his Lax–Wendroff TVD scheme [13]. We also call this limiter Superbee, indicated by q^s. In Fig. 1, it is seen that the most compressive TVD-satisfying limiter function is

$$q(r)=\begin{cases}0, & r\leqslant 0\\ kr, & 0<r\leqslant 2/k\\ 2, & r>2/k.\end{cases} \tag{2.19}$$

Usually this limiter is too compressive. It will turn the sine wave into a square wave when it is applied to the linear wave equation (see Section 4). This limiter is thus named "Supercompressive," denoted by q^p. Another limiter which is of particular interest in this paper is

$$q(r)=\begin{cases}0, & r\leqslant 0\\ kr, & 0<r\leqslant 1/k\\ 1, & r>1/k.\end{cases} \tag{2.20}$$

When fully implicit schemes are employed, $k\Rightarrow\infty$. That means the resulant scheme possesses no dissipation away from local extrema.

3. Comparison of Osher–Chakravarthy and Yee TVD Schemes

3.1. *Osher–Chakravarthy Scheme*

In [3], Osher–Chakravarthy derived a family of high-order TVD schemes. For the linear scalar equation (2.8), the numerical flux function takes the form

$$h_{j+1/2}=cu_j+\frac{1+\varphi}{4}[\tilde{d}f_{j+1/2}]+\frac{1-\varphi}{4}[\hat{d}f_{j-1/2}], \tag{3.1a}$$

where φ is a parameter and $-1 \leqslant \varphi \leqslant 1$. The symbols $\tilde{}$ and $\hat{}$ shown over df denote flux-limited values of df and are computed as

$$\begin{aligned} \tilde{df}_{j+1/2} &= \text{minmod}(c\,\Delta u_{j+1/2}, \beta c\,\Delta u_{j-1/2}) \\ \hat{df}_{j-1/2} &= \text{minmod}(c\,\Delta u_{j-1/2}, \beta c\,\Delta u_{j+1/2}), \end{aligned} \tag{3.1b}$$

where the minmod function is defined as

$$\text{minmod}(x, y) = \begin{cases} 0, & xy < 0 \\ \text{sign}(x)\,\min(|x|, |y|), & xy \geqslant 0. \end{cases} \tag{3.2}$$

Actually, we can rewrite (3.1) as (2.9a) with

$$q(r_j) = \frac{1+\varphi}{2}\psi(r_j) + \frac{1-\varphi}{2} r_j \psi\left(\frac{1}{r_j}\right), \tag{3.3a}$$

where

$$\psi(r_j) = \text{minmod}(1, \beta r_j). \tag{3.3b}$$

It is now necessary to decide the range of β which makes the scheme TVD.

Obviously, the following can be obtained:

$$q(r) = \begin{cases} 0, & r \leqslant 0 \\ \dfrac{1+\varphi}{2}\beta r + \dfrac{1-\varphi}{2} r, & 0 < r \leqslant 1/\beta \\ \dfrac{1+\varphi}{2} + \dfrac{1-\varphi}{2} r, & 1/\beta < r < \beta \\ \dfrac{1+\varphi}{2} + \dfrac{1-\varphi}{2}\beta, & r \geqslant \beta. \end{cases} \tag{3.4}$$

So, clearly,

$$\max(q(r)) = \frac{1+\varphi}{2} + \frac{1-\varphi}{2}\beta \tag{3.5a}$$

and

$$\max(q(r)/r) = \frac{1+\varphi}{2}\beta + \frac{1-\varphi}{2}. \tag{3.5b}$$

Now the follwing should be satisfied:

$$\max(q(r)) \leqslant 2 \tag{3.6a}$$

and

$$\max(q(r)/r) \leqslant \frac{2}{\lambda c(1-\eta)} - 2 = k. \tag{3.6b}$$

Thus it is required that

$$\beta \leqslant \min\left(\frac{3-\varphi}{1-\varphi}, \frac{2k-1+\varphi}{1+\varphi}\right). \tag{3.7}$$

For $\eta = 1$, i.e., the backward Euler scheme, $k \to \infty$, then

$$\beta_{\max} = \frac{3-\varphi}{1-\varphi}. \tag{3.8}$$

For $\eta = 0$, i.e., the explicit scheme,

$$k = 2(1/v - 1), \tag{3.9}$$

where

$$v = c\lambda. \tag{3.10}$$

Thus, k depends on v, and so does $\beta_{\max}$. If we fix the CFL number to, say, $\frac{1}{3}$, we have

$$k = 4 \tag{3.11a}$$

and then

$$\beta_{\max} = \min\left(\frac{3-\varphi}{1-\varphi}, \frac{7+\varphi}{1+\varphi}\right). \tag{3.11b}$$

Table I shows the maximum β for different values of φ ($v = \frac{1}{3}$).

For each value of φ, the respective limiter function is plotted in Fig. 2. It is shown that all the limiters are within the upwind-biased second-order domain.

TABLE I

$\beta_{\max}$ for Explicit Osher–Chakravarthy Scheme with $v = \frac{1}{3}$

φ	Underlying scheme	$\beta_{\max}$
1/3	Third-order	4
−1	Fully upwind	2
0	Fromm's	3
1/2	Low TE second-order	5
1	Central	4
−1/3	Un-named	5/2

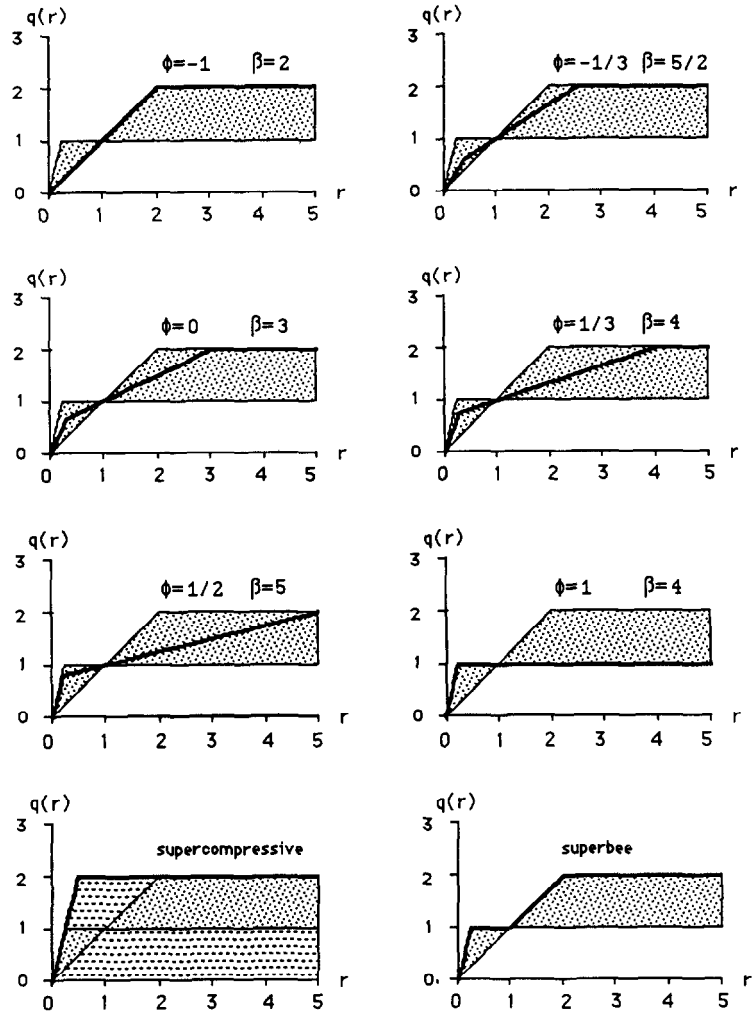

FIG. 2. Limiter functions.

3.2. *Yee Scheme*

In [4], Yee generalized the works of Davis [5] and Roe [6] and introduced the symmetric TVD scheme. Again, for the scalar wave equation, the numerical flux function is

$$h_{j+1/2} = \tfrac{1}{2}c(u_{j+1} + u_j) - \tfrac{1}{2}c(1 - Q)\,\Delta u_{j+1/2} \tag{3.12a}$$

with

$$Q = Q(r^+_{j+1/2}, r^-_{j+1/2}) \tag{3.12b}$$

and

$$r^+_{j+1/2} = \frac{\Delta u_{j+3/2}}{\Delta u_{j+1/2}}, \qquad r^-_{j+1/2} = \frac{\Delta u_{j-1/2}}{\Delta u_{j+1/2}}. \tag{3.13}$$

It is clear that $r^-_{j+1/2}$ is identical to the previously defined r_j. Yee's typical limiter functions are

$$Q(r^+, r^-) = \text{minmod}(r^+, r^-, 1) \tag{3.14a}$$

$$Q(r^+, r^-) = \text{minmod}(1, r^+) + \text{minmod}(1, r^-) - 1 \tag{3.14b}$$

$$Q(r^+, r^-) = \text{minmod}(2, 2r^+, 2r, 0.5(r^+ + r^-)). \tag{3.14c}$$

The difference in the definition of the limiter functions is obvious. Yee's limiters are equally dependent on the upwind and downwind gradients which makes the name symmetric TVD natural. Comparing (3.12) and (2.9), we see that

$$q = Q(r^+_{j+1/2}, r^-_{j+1/2}). \tag{3.15}$$

Obviously, with a proper choice of CFL-like conditions, that is, $\lambda c \leqslant \text{const}$, these limiters satisfy the conditions (2.15). If the backward Euler scheme is used for time discretisation, the Yee scheme is unconditionally TVD. It needs to be pointed out that Q in (3.14b) can be negative. So Q should return to zero once a negative value is obtained from (3.14b). Because of the symmetric property of Yee's TVD scheme, limiter functions (3.14) introduced extra dissipation even if the solution is relatively smooth. Take limiter (3.14a), for example. If $0 < r^+ < r^- < 1$, then Q will be equal to r^+ instead of r^-. That means

$$q < r_j. \tag{3.16}$$

Hence this function lies outside of the upwind-biased second-order TVD region. The result of this is that it includes extra dissipation because the dissipation coefficient $(1 - r^+)$ is larger than $(1 - r^-)$. The extra amount of dissipation the Yee scheme possesses usually does no harm to the solution of Euler equations. However, when it is used to solve the Navier–Stokes equations, especially for problems at high Reynolds number, caution needs be exercised to ensure that the numerical dissipation does not exceed the physical dissipation. Otherwise, the solution would be meaningless.

Remedies to make Yee's TVD less dissipative while maintaining its TVD property are now presented. The limiter functions are formed according to the specific wave direction; i.e.,

$$Q(r^+, r^-) = \frac{1 + \text{sign}(c)}{2} \text{minmod}(1, r^-) + \frac{1 - \text{sign}(c)}{2} \text{minmod}(1, r^+) \tag{3.17a}$$

$$Q(r^+, r^-) = \frac{1 + \text{sign}(c)}{2} \text{minmod}(1, \omega r^-) + \frac{1 - \text{sign}(c)}{2} \text{minmod}(1, \omega r^+), \tag{3.17b}$$

where $1 < \omega < \infty$ for fully implicit schemes. Limiters (3.17a) and (3.17b) are called MY1 and MY2, respectively. MY2 is expected to be very useful for viscous flow calculations. Numerical experiments as outlined in the next section do show that these modified Yee schemes give better results.

4. Discussion of Numerical Results

4.1. The first numerical experiment is performed on the linear wave equation (2.8). The explicit schemes ($\eta = 0$) of Osher–Chakravarthy and Yee are employed. As a result, the schemes are only first-order accurate in time but second-order in space. However, some of the results obtained are strikingly good. For the

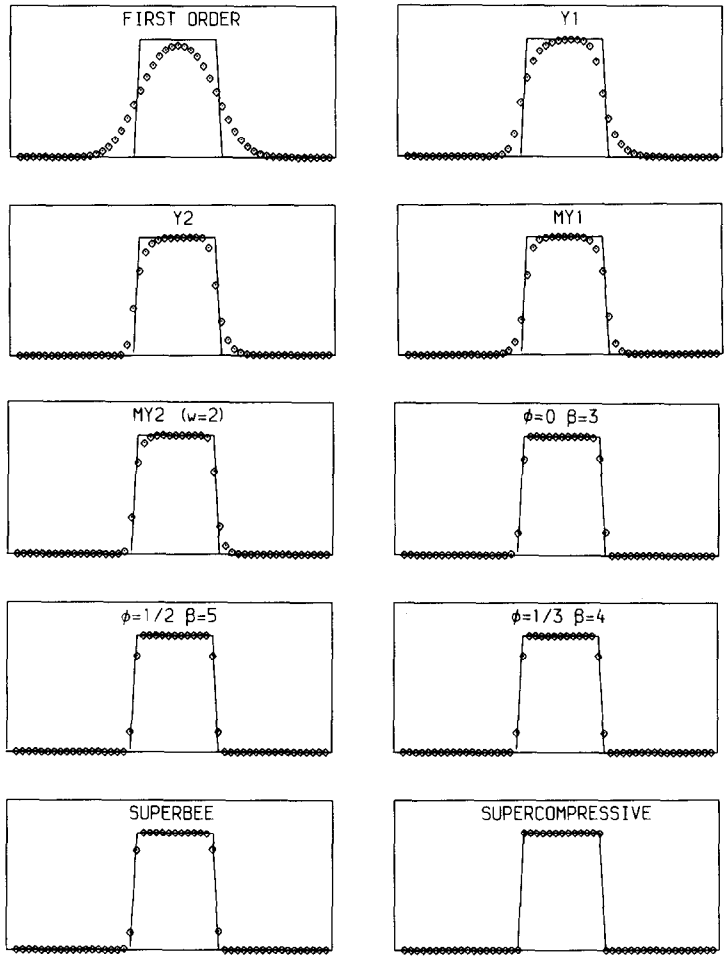

FIG. 3. Square wave propagation.

following calculations, a fixed CFL number of $\frac{1}{3}$ is used throughout. Fifty-one time step for the square-wave calculation, and 27 time steps for sine wave calculation, are propogated.

For the Yee scheme, two limiters are employed, i.e., those given by (3.14a) and (3.14c). They are called Y1 and Y2, respectively. For the Osher–Chakravarthy scheme, different values of φ are selected and $\beta_{\max}$ is used.

Also present are results using Superbee and Supercompressive. For the linear advection problem, the MY1 limiter as modified in Section 3 is identical to the Osher–Chakravarthy scheme with $\varphi = 1$ and $\beta = 1$.

Figure 3 shows results for the square wave calculation. The solid line represents the exact solution. It can be seen that the Supercompressive limiter gives the best

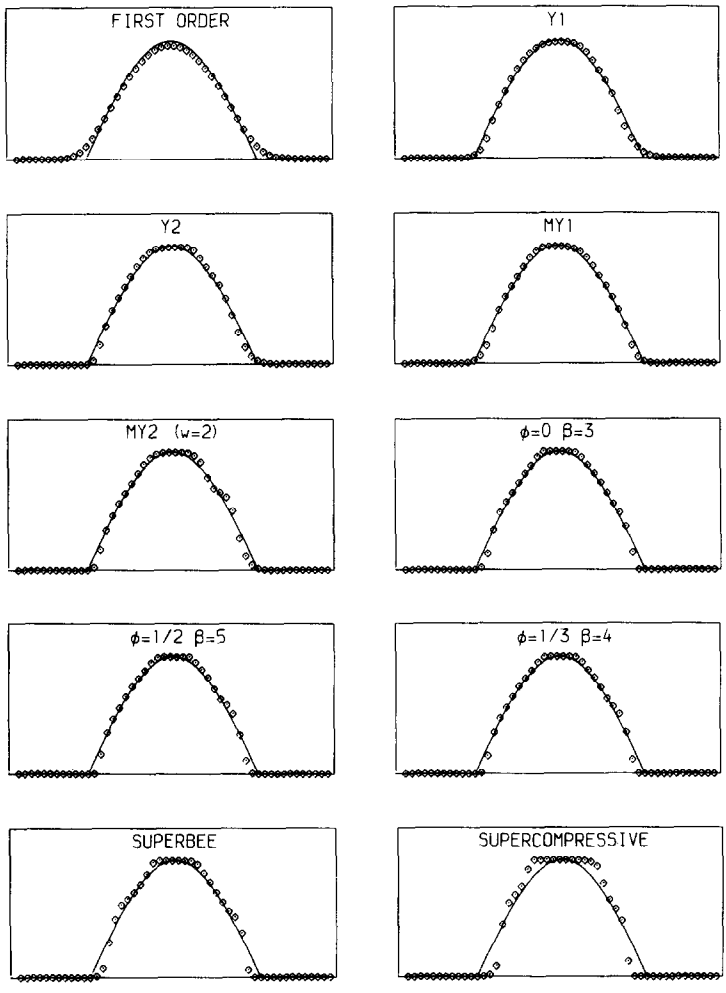

FIG. 4. Sine wave propagation.

result and cannot be differentiated from the exact solution. The next best result comes from the solution utilizing Superbee, followed by the Osher–Chakravarthy scheme with $\varphi = \frac{1}{2}$, $\beta = 5$ and $\varphi = \frac{1}{3}$, $\beta = 4$, respectively.

As expected, the Osher–Chakravarthy scheme with any value of φ gives better results than the Yee scheme as far as resolution is concerned. Comparing the results from Y1, Y2 and the results from the Osher–Chakravarthy scheme, it is seen clearly that Yee scheme gives the most dissipative results downstream of steep gradients. This is due to the fact that $q(r) < r$ at such places. The modified Yee schemes give superior results than the original schemes. It is also obvious that Y2 gives better results than Y1 and the Yee scheme gives better results than the first-order scheme.

Figure 4 illustrates the results for the sine wave calculation. It is seen that both Supercompressive and Superbee are over compressive. It is also found that any value of φ, $\beta_{\max}$ gives a slightly "squared" sine wave as can be seen in Fig. 4. It appears that the results given by Y1 and Y2 have a better agreement with the exact solution than those given by the Osher–Chkravarthy scheme. The reason behind this phenomenon, is believed to be that the time-stepping approach is only first-order accurate so that a negative second-order dissipation term is embedded. This explains the slight "squaring" effect on top of the sine wave even in the results given by MY1 and MY2.

4.2. The second test problem is the quasi-one-dimensional nozzle problem. The governing equation for this problem is

$$\frac{\partial U}{\partial t} + \frac{\partial F(U)}{\partial x} - H(U) = 0, \tag{4.1}$$

where

$$U = \kappa \begin{bmatrix} \rho \\ \rho v \\ e \end{bmatrix}, \qquad F = \kappa \begin{bmatrix} \rho v \\ (p + \rho v^2) \\ (e + p)v \end{bmatrix}, \qquad H(U) = \begin{bmatrix} 0 \\ p\,\partial\kappa/\partial x \\ 0 \end{bmatrix} \tag{4.2}$$

with κ, the cross area of the nozzle, a function of x. The configuration considered (see Fig. 5) is a divergent nozzle [10] with

$$\kappa(x) = 1.398 + 0.347 \tanh(0.8x - 4). \tag{4.3}$$

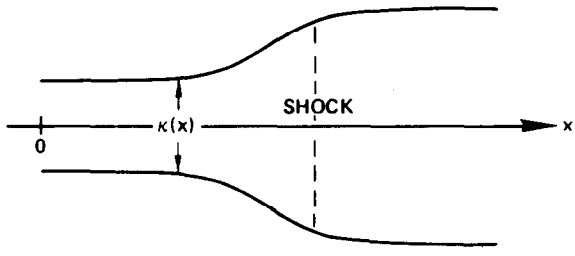

FIG. 5. Divergent nozzle.

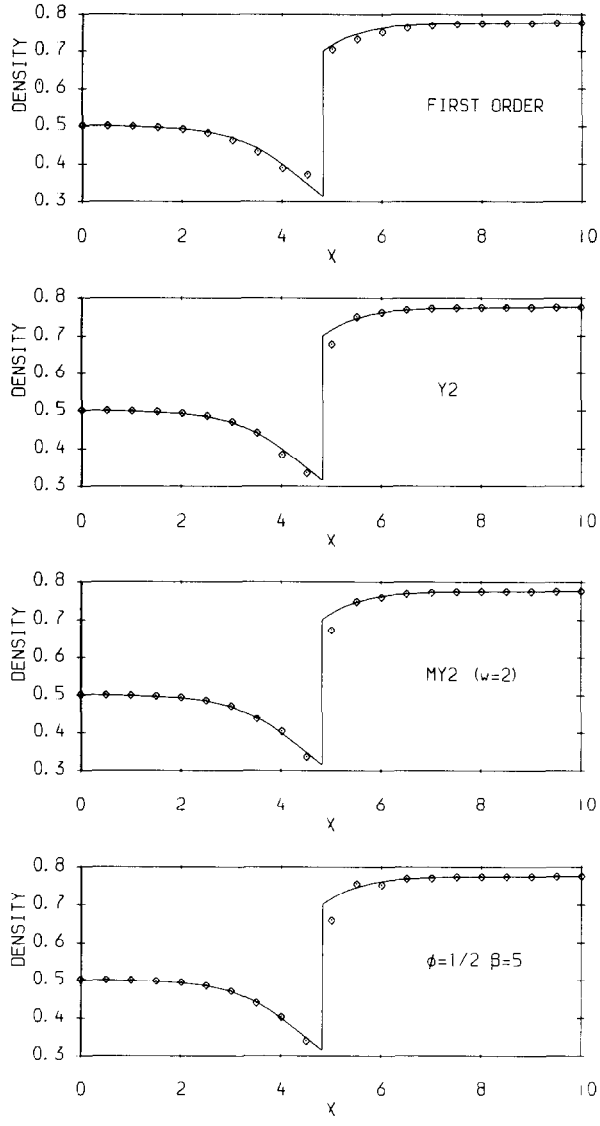

FIG. 6. Density distribution.

The flow condition is supersonic at the entrance and subsonic at the exit, divided by a normal shock. The computational domain is selected to be $0 \leqslant x \leqslant 10$, and a very coarse even-spaced mesh of $\Delta x = 0.5$ is used to evaluate the resolution capacity of the scheme. The schemes are extended to a system of conservation laws according to the technique employed in [10]. Roe's approximate Riemann solver is employed to define the local characteristics. For objective comparison no entropy

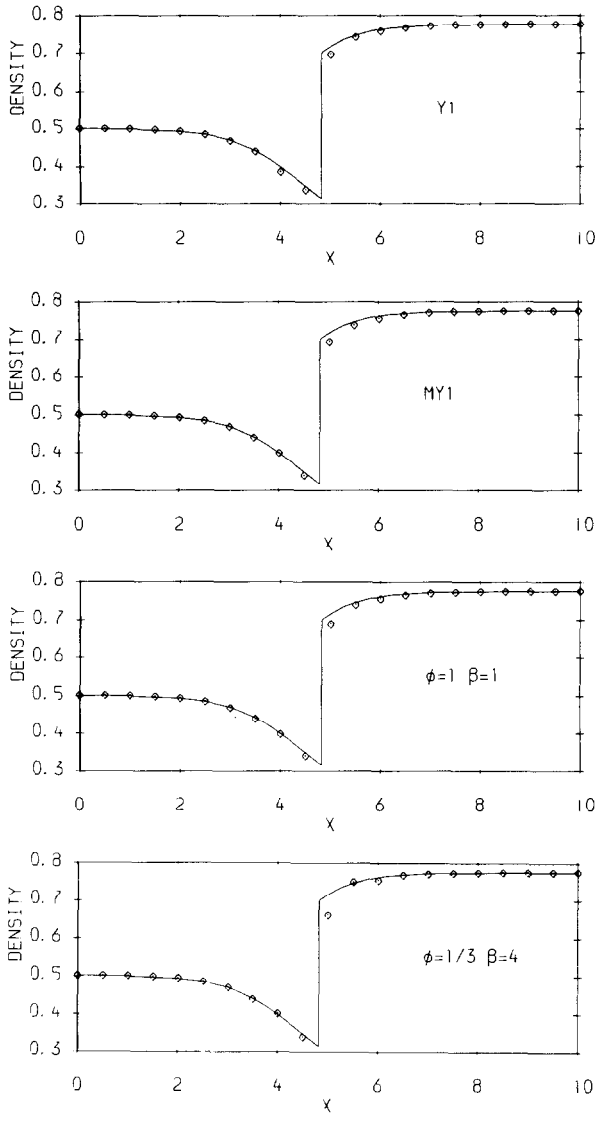

FIG. 6—*Continued*

enforcement is applied. An implicit method using backward Euler scheme in time is utilised. For more details, see [1, 10].

Figure 6 presents the results for the Yee, modified Yee and Osher–Chakravarthy schemes with different choices of limiters and relevant parameters. In the experiments with $\varphi = \frac{1}{2}$ and $\varphi = \frac{1}{3}$, it is found that $\beta_{\max}$ will give slightly oscillatory results. It is speculated that these schemes are over compressive with the result that instability has set in resulting in the overshoot near the shock wave. The upstream

part of the shock is seen to be smeared by the first-order scheme. All the rest of the schemes demonstrated almost equally good quality in their shock resolution capacities.

4.3. The last experiment chosen is to test the ability of the different TVD schemes to resolve a boundary layer. For this purpose, a shock wave/boundary layer interaction problem is selected. The flowfield representing this interaction is sketched in Fig. 7. The oblique shock wave is generated externally and is incident upon a boundary layer on a flat plate. If the shock is strong enough, the boundary layer will separate from the surface of the plate and reattach downstream. The separation region is a demanding one to calculate and therefore serves as a good test for a numerical method. The computational domain is chosen to be $-0.02 \leqslant x \leqslant 0.3$ and $0.0 \leqslant y \leqslant 0.1215$. The grid is composed of 33×33 points. The Reynolds number based on a reference length of 0.16 is taken to be 296,000. The free stream Mach number is 2.0. The flat plate is introduced from $x = 0.03$. A shock is imposed at $x = 0$, $y = 0.1215$ such that it slopes to the flat plate at 32.6°. The governing equations are the two-dimensional Navier–Stokes equations,

$$\frac{\partial U}{\partial t} + \frac{\partial E}{\partial x} + \frac{\partial F}{\partial y} = \frac{\partial E_v}{\partial x} + \frac{\partial F_v}{\partial y}, \tag{4.4}$$

where

$$U = \begin{bmatrix} \rho \\ \rho u \\ \rho v \\ e \end{bmatrix}, \quad E = \begin{bmatrix} \rho u \\ \rho u^2 + p \\ \rho uv \\ (e+p)u \end{bmatrix}, \quad F = \begin{bmatrix} \rho v \\ \rho uv \\ \rho v^2 + p \\ (e+p)v \end{bmatrix} \tag{4.5}$$

$$E_v = \frac{1}{\mathrm{Re}} \begin{bmatrix} 0 \\ \tau_{xx} \\ \tau_{xy} \\ u\tau_{xx} + v\tau_{xy} + q_x \end{bmatrix}, \quad F_v = \frac{1}{\mathrm{Re}} \begin{bmatrix} 0 \\ \tau_{xy} \\ \tau_{yy} \\ u\tau_{xy} + v\tau_{yy} + q_y \end{bmatrix}$$

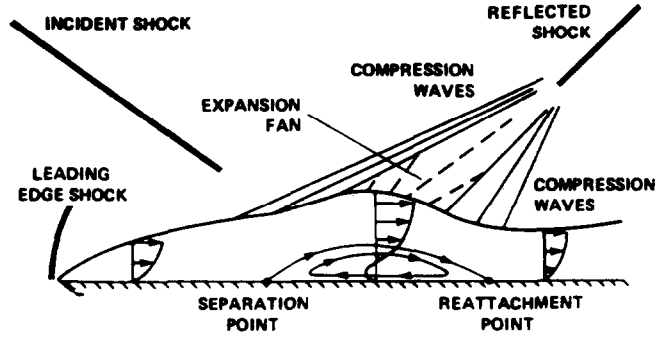

FIG. 7. Sketch for shock boundary layer interaction.

with

$$
\begin{aligned}
e &= \frac{p}{\gamma - 1} + \frac{\rho}{2}(u^2 + v^2) \\
\tau_{xx} &= \frac{2}{3}\mu\left(2\frac{\partial u}{\partial x} - \frac{\partial v}{\partial y}\right) \\
\tau_{xy} &= \mu\left(\frac{\partial u}{\partial y} + \frac{\partial v}{\partial x}\right) \\
\tau_{yy} &= \frac{2}{3}\mu\left(2\frac{\partial v}{\partial y} - \frac{\partial u}{\partial x}\right) \\
q_x &= \frac{\mu}{(\gamma - 1) M_\infty^2 \,\mathrm{Re}\,\mathrm{Pr}} \frac{\partial T}{\partial x} \\
q_y &= \frac{\mu}{(\gamma - 1) M_\infty^2 \,\mathrm{Re}\,\mathrm{Pr}} \frac{\partial T}{\partial y},
\end{aligned}
\tag{4.6}
$$

where μ is the coefficient of viscosity.

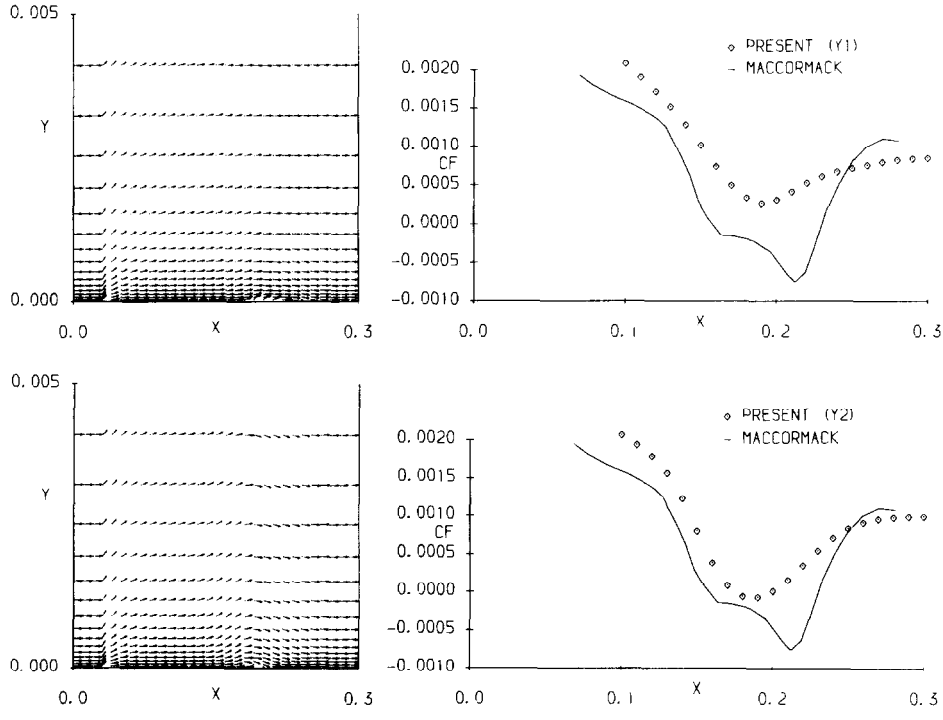

FIG. 8. Plots of velocity direction and skin friction coefficient of the Yee scheme.

Out of this, the subset

$$\frac{\partial U}{\partial t}+\frac{\partial E}{\partial x}+\frac{\partial F}{\partial y}=0 \tag{4.7}$$

is the Euler equations of inviscid compressible flow. In the numerical experiment, the flux vectors E and F are discretised using a TVD scheme, and the viscous terms (E_v and F_v) are discretised using central differences. Roe's approximate Riemann solver is employed to define the local characteristics. No entropy modification is employed. Then the implicit factorization method is utilised to solve the resultant system. See [10, 11] for details.

Figures 8, 9, and 10 show plots of the velocity direction and skin friction coefficient for calculations with the Yee, modified Yee, and Osher–Chakravarthy schemes, respectively, since these two parameters are the most distinguishing. The results are compared with the results from MacCormack [12]. From the velocity plot, we can see clearly that both the modified Yee scheme and the Osher–Chakravarthy scheme resolved the separation very well while the Yee scheme did not. Y1 limiter gave an unseparated flow pattern. Y2 gave a slightly separated flow, but is not at all satisfactory. It is noticed that MY2 is a very

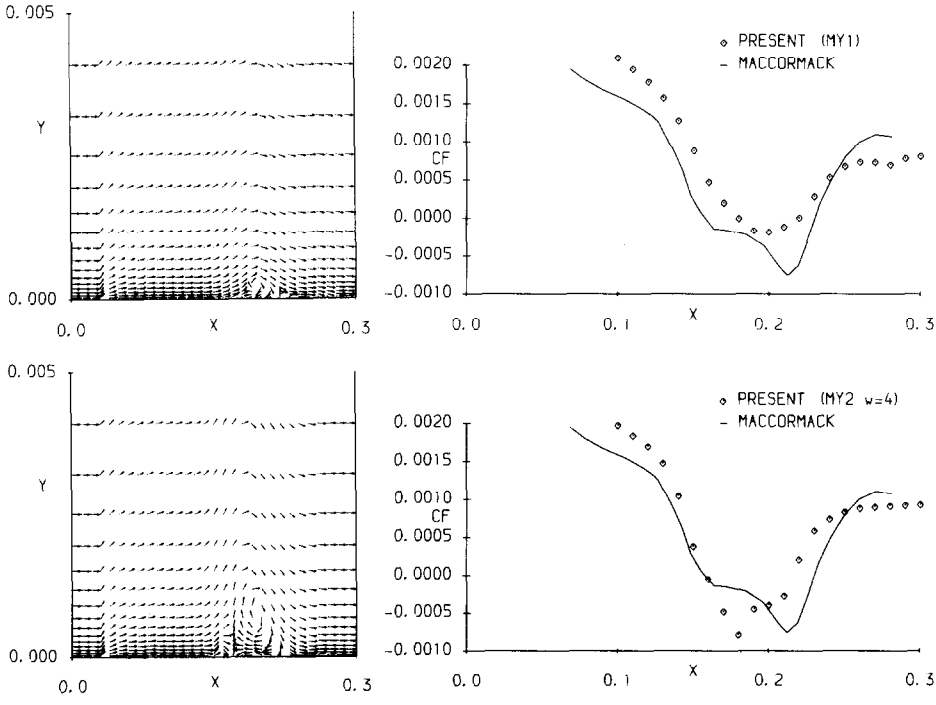

FIG. 9. Plots of velocity direction and skin friction coeffient of the modified Yee scheme.

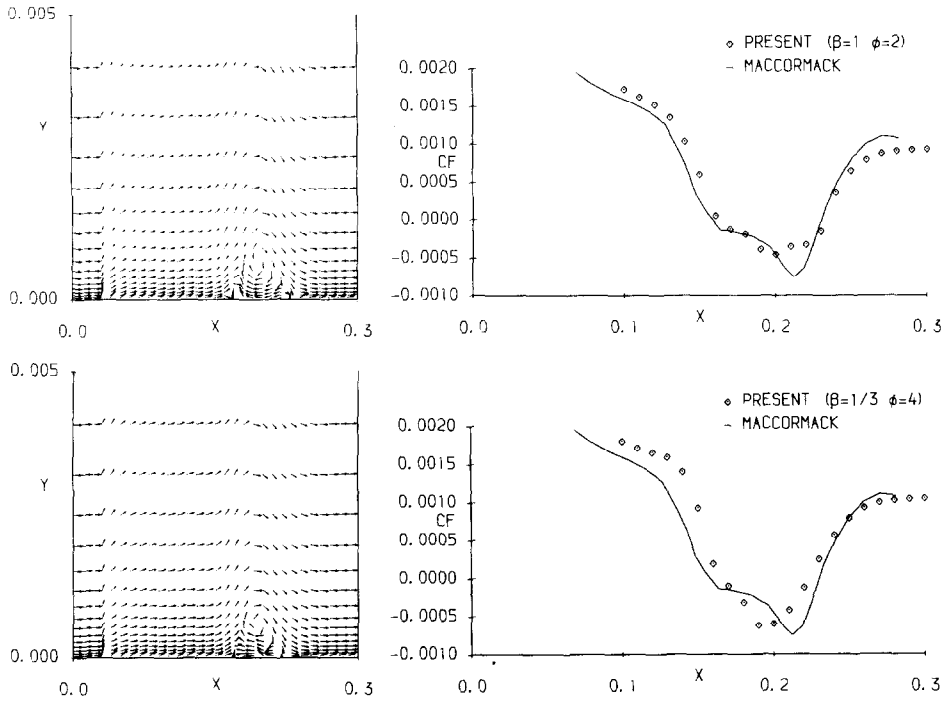

FIG. 10. Plots of velocity direction and skin friction coefficient of the Osher–Chakravarthy scheme.

promising limiter to attack the viscous flows at high Reynolds number. It is much better than MY1. In the test, the same basic computer code was used. Only the inviscid flux subroutine was changed. Thus it seems reasonable to conclude that the original Yee scheme did introduce extra viscosity and that this viscosity exceeded the physical viscosity such that unrepresentative results are obtained.

5. Concluding Remarks

Although TVD schemes have been applied in inviscid flow solutions very successfully, their capacity to resolve viscous shear layers is still quite unclear. By unifying and comparing two TVD schemes, namely the Osher–Chakravarthy and the Yee scheme, we see that the former is much less dissipative than the latter. This property may not affect the inviscid flow region very much. However, when a viscous solution at high Reynolds number is sought, they could result in dramatically different solutions. The paper demonstrates that the dissipation imbedded in the schemes may be the cause. When physical dissipation is overwhelmed by numerical dissipation, the solution will be unrepresentative. A "numerical solution" in this case will be valueless. The goal then is to resolve the problem with the least numerical

dissipation possible. The modified Yee schemes are therefore suggested to approach that goal.

ACKNOWLEDGMENTS

The first author is sponsored by the SBFSS administered by the Britisch Council. Some help from Mr. Zhilin Li is appreciated by the authors.

REFERENCES

1. A. HARTEN, *J. Comput. Phys.* **49**, 357 (1983).
2. P. K. SWEBY, *SIAM J. Numer. Anal.* **21**, 995 (1984).
3. S. OSHER AND S. R. CHAKRAVARTHY, ICASE Report No. 84-44, September 1984, NASA Langley Research Center, Hampton, Virginia.
4. H. C. YEE, *J. Comput. Phys.* **68**, 151 (1987).
5. S. F. DAVIS, "TVD Finite Difference Schemes and Artificial Viscosity," ICASE Report No. 84-20, June 1984 (unpublished).
6. P. L. ROE, "General Formulation of TVD Lax–Wendroff Schemes," ICASE Report No. 84-53, October 1984 (unpublished).
7. Y. TAKAKURA, T. ISHIGURO, AND S. OGAWA, in *Proceedings, AIAA Eighth Computational Fluid Dynamics Conference, Honolulu, Hawaii*, 1987, AIAA-87-1151.
8. P. L. ROE, *J. Comput. Phys.* **43**, 357 (1983).
9. S. R. CHAKRAVARTHY, "High Resolution Upwind Formulations for Hyperbolic Conservation Laws," in *Lecture Notes for Computational Fluid Dynamics, von-Karman Institute for Fluid Dynamics, March* 1988.
10. H. C. YEE, R. F. WARNING, AND A. HARTEN, *J. Comput. Phys.* **57**, 327 (1985).
11. T. H. PULLIAM AND J. L. STEGER, AIAA-85-0360, January 1985 (unpublished).
12. R. W. MACCORMACK, *AIAA J.* **20**, 1275 (1982).
13. P. L. ROE, in *Proceedings, AMS–SIAM Summer Seminar on Large-Scale Computation in Fluid Mechanics*, 1983, edited by B. E. Engquist *et al.*, Lectures in Applied Mathematics, Vol. 22 (Amer. Math. Soc., Providence, RI, 1985), p. 163.